A comparison of nonstaggered compact FDTD schemes for the 3D wave equation

Kowalczyk, K., & Van Walstijn, M. (2010). A comparison of nonstaggered compact FDTD schemes for the 3D wave equation. 197-200. Paper presented at EEE International Conference on Acoustics, Speech and Signal Processing (ICASSP 2010), Dallas, United States.DOI: 10.1109/ICASSP.2010.5496043

A COMPARISON OF NONSTAGGERED COMPACT FDTD SCHEMES FOR THE 3D WAVE EQUATION

Konrad Kowalczyk[*]

Multimedia Communications and Signal Processing
University of Erlangen-Nuremberg, Germany
kowalczyk@lnt.de

Maarten van Walstijn

Sonic Arts Research Centre
Queen's University of Belfast, UK
m.vanwalstijn@qub.ac.uk

ABSTRACT

This paper aims at providing a better insight into the 3D approximations of the wave equation using compact finite-difference time-domain (FDTD) schemes in the context of room acoustic simulations. A general family of 3D compact explicit and implicit schemes based on a nonstaggered rectilinear grid is analyzed in terms of stability, numerical error, and accuracy. Various special cases are compared and the most accurate explicit and implicit schemes are identified. Further considerations presented in the paper include the direct relationship with other numerical approaches found in the literature on room acoustic modeling such as the 3D digital waveguide mesh and Yee's staggered grid technique.

Index Terms— Acoustic propagation, acoustic signal processing, architectural acoustics, finite-difference time-domain (FDTD) methods

1. INTRODUCTION

The finite-difference time-domain (FDTD) technique has numerous practical applications in the area of auralization and architectural design of acoustic spaces such as auditoria, churches, listening rooms, and concert halls [1]. Since real acoustic spaces are three-dimensional, the numerical solution of the 3D wave equation is a primary objective in room acoustic simulation.

A numerical artifact of the FDTD technique is that high frequencies propagate at a lower speed than the real sound wave velocity (which is constant for all frequencies in a nondispersive medium such as air). Furthermore, this error is often direction-dependent. Therefore, the aim of this paper is to indicate those FDTD schemes for which this artifact is considerably reduced. Various grid topologies have been proposed in the past in the context of FDTD and digital waveguide mesh (DWM) room acoustic simulations, including the standard rectilinear stencil (utilized by the standard leapfrog scheme [2], Yee's staggered scheme [1], and the rectangular DWM [3]), the cubic close-packed stencil [3],[4], the octahedral grid topology [3],[4], and the interpolated stencil [5], [6]. Implicit schemes, that are less known in the context of acoustics and audio, can also be applied. As explained in this paper, all of these schemes can be captured in a single formulation with a set of free numerical parameters that specify any one particular scheme. For implicit cases this formulation allows efficient implementation using alternating direction implicit (ADI) technique [7], where the required 3D matrix inversion is reduced to a set of three 1D matrix inversion problems that can be computed speedily using the Thomas algorithm [2]. Because a long term aim of our work is to simulate rooms with moving sound sources and receivers, we exclude the use of frequency warping techniques (that require offline computations [5]) in the analysis of schemes.

[*]The first author performed the work while at Queen's University Belfast.

2. 3D COMPACT SCHEME FORMULATION

Wave propagation in a 3D acoustic space is defined by conservation of momentum and conservation of mass equations, which in combination yield the 3D wave equation [8]

$$\frac{\partial^2 p}{\partial t^2} = c^2 \left(\frac{\partial^2 p}{\partial x^2} + \frac{\partial^2 p}{\partial y^2} + \frac{\partial^2 p}{\partial z^2} \right), \tag{1}$$

where c denotes sound velocity and p is the pressure variable. The 3D compact implicit FDTD scheme approximating (1) in the form that enables an alternating direction implicit implementation can be expressed as [7]

$$\begin{aligned}(1+a\delta_x^2)(1+a\delta_y^2)(1+a\delta_z^2)\delta_t^2 p^n_{l,m,i} = \lambda^2[&(\delta_x^2+\delta_y^2+\delta_z^2)\\ &+b(\delta_x^2\delta_y^2+\delta_y^2\delta_z^2+\delta_x^2\delta_z^2)\\ &+c\delta_x^2\delta_y\delta_z]p^n_{l,m,i},\end{aligned} \tag{2}$$

where λ denotes the Courant number, a, b, and c are free parameters, n denotes a time index, and l, m, and i are spatial indices in x-, y-, and z-direction, respectively. An update formula for a grid point is obtained by substituting respective centered finite-difference operators into (2), the example operator in z-direction given as $\delta_z^2 p^n_{l,m,i} \equiv p^n_{l,m,i+1} - 2p^n_{l,m,i} + p^n_{l,m,i-1}$, where $p^{n+1}_{l,m,i}$ is a pressure variable. Note that an implicit scheme results for $a \neq 0$. The most efficient splitting formula for the 3D ADI method has been proposed in [7]

$$(1+a\delta_x^2)p^{n+1*}_{l,m,i} = \frac{\lambda^2}{a}[-1+(a-b)(\delta_y^2+\delta_z^2)]p^n_{l,m,i}, \tag{3}$$

$$(1+a\delta_y^2)p^{n+1**}_{l,m,i} = p^{n+1*}_{l,m,i} + \frac{\lambda^2}{a}(b-a)\delta_y^2 p^n_{l,m,i}, \tag{4}$$

$$(1+a\delta_z^2)\delta_t^2 p^n_{l,m,i} = p^{n+1**}_{l,m,i} + \frac{\lambda^2}{a}(1+b\delta_z^2)p^n_{l,m,i}, \tag{5}$$

where $p^{n+1*}_{l,m,i}$ and $p^{n+1**}_{l,m,i}$ are intermediate pressure variables. This splitting formula requires that $c = ab$, and hence the number of implicit schemes' free parameters is reduced to two. The computational procedure consists of three subsequent stages in which intermediate values are calculated row by row in all three respective propagation directions. The resulting 1D matrix inversions can be implemented efficiently using the Thomas algorithm [2].

3. NUMERICAL STABILITY

For FDTD stability analysis, a single-frequency plane-wave solution of the discrete wave equation is usually assumed

$$p^n_{l,m,i} = p_0\, e^{snT} e^{-\hat{k}_x lX} e^{-\hat{k}_y mX} e^{-\hat{k}_z iX}, \tag{6}$$

where p_0 is the pressure amplitude, $s = \sigma + j\omega$ denotes complex frequency, X is the grid spacing, $T = 1/f_s$ is the time step, and discrete directional wavenumbers are given as $\hat{k_x} = \hat{k}\cos\theta\cos\phi$, $\hat{k_y} = \hat{k}\sin\theta\cos\phi$, and $\hat{k_z} = \hat{k}\sin\phi$, respectively. Expressing finite-difference operators as

$$\begin{aligned}\delta_t^2 p^n_{l,m,i} &= \left(z - 2 + z^{-1}\right) p^n_{l,m,i}, \\ &= -4\sin^2(\omega T/2)\, p^n_{l,m,i},\end{aligned} \tag{7}$$

$$\delta_x^2 p^n_{l,m,i} = -4\sin^2(\hat{k}_x X/2)\, p^n_{l,m,i}, \tag{8}$$

for all spatial directions, and substituting them into (2) leads to

$$z + 2B(s_x, s_y, s_z) + z^{-1} = 0, \tag{9}$$

where $z = e^{sT}$, and where we introduced the new variables $s_x = \sin^2(\hat{k}_x X/2)$, $s_y = \sin^2(\hat{k}_y X/2)$, and $s_z = \sin^2(\hat{k}_z X/2)$, and

$$B(s_x, s_y, s_z) = 2\lambda^2 F(s_x, s_y, s_z) - 1, \tag{10}$$

in which

$$\begin{aligned}F(s_x, s_y, s_z) = [(s_x + s_y + s_z) - 4b(s_x s_y + s_x s_z + s_y s_z) \\ +16c s_x s_y s_z] \,/\, [1 - 4a(s_x + s_y + s_z) \\ +16a^2(s_x s_y + s_x s_z + s_y s_z) - 64a^3 s_x s_y s_z].\end{aligned} \tag{11}$$

Von Neumann analysis - that is typically applied in FDTD literature for investigating numerical stability [2, 9] - seeks a stability bound on λ so that no growing solutions exist, which can be expressed as $|z| \leq 1$. For stability analysis, it is sufficient to consider real-valued wavenumbers only [6, 10], i.e., in the range $-\pi/X \leq \hat{k}_x, \hat{k}_y, \hat{k}_z \leq \pi/X$, which from (9) can be formulated as

$$\lambda^2 \leq \frac{1}{F(s_x, s_y)}. \tag{12}$$

Noting that s_x, s_y, s_z are always in the range of $[0, 1]$, one obtains

$$F_{\max} = \max\left(\frac{1}{1-4a}, \frac{2-4b}{1-8a+16a^2}, \frac{3-12b+16c}{1-12a+48a^2-64a^3}\right). \tag{13}$$

Thus the stability condition for 3D compact FDTD schemes is

$$\lambda^2 \leq \min\left(1 - 4a, \frac{1-8a+16a^2}{2-4b}, \frac{1-12a+48a^2-64a^3}{3-12b+16c}\right), \tag{14}$$

which finally leads to the following conditions on free parameters

$$a \leq \frac{1}{4}, \quad b \leq \frac{1}{2}, \quad c \geq \frac{1}{16}(12b - 3). \tag{15}$$

4. NUMERICAL DISPERSION RELATION

As a measure of the dispersion error, the relative phase velocity (defined as the ratio of the effective numerical wave speed given as $\omega/\hat{k}$ over the real wave speed) is typically applied [9]. Substituting (7) into (9), and next rewriting it explicitly for ω yields

$$\omega = \frac{2}{T}\arcsin\left(\lambda\sqrt{F(s_x, s_y, s_z)}\right), \tag{16}$$

Table 1. Special cases of 3D compact FDTD schemes.

scheme	a	b	c	λ	l. cutoff
SLF	0	0	0	$\frac{1}{\sqrt{3}}$	0.196
OCTA	0	$\frac{1}{2}$	$\frac{1}{4}$	1	0.25
CCP	0	$\frac{1}{4}$	0	1	0.333
IDWM	0	0.2034	0.0438	$\frac{1}{\sqrt{3}}$	0.196
IISO	0	$\frac{1}{6}$	0	$\frac{3}{4}$	0.333
IISO2	0	$\frac{1}{6}$	$\frac{1}{48}$	$\frac{3}{4}$	0.333
IWB	0	$\frac{1}{4}$	$\frac{1}{16}$	1	0.5
FOA	0.0387	$\frac{1}{6}$	0.0064	$\sqrt{3}-1$	0.242

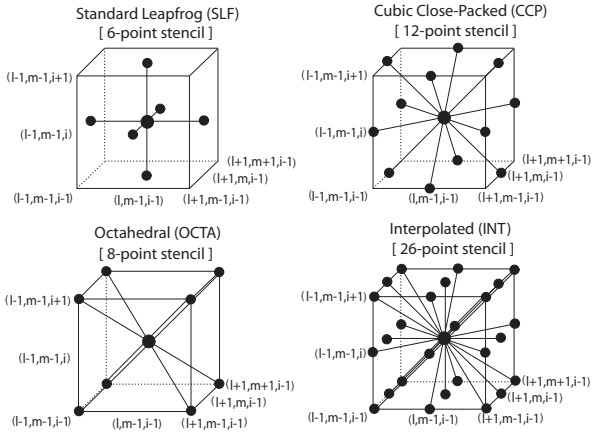

Fig. 1. Compact FDTD stencils for the 3D standard leapfrog, the octahedral, the cubic close-packed, and the 3D interpolated schemes.

which leads to the analytic formula for the relative phase velocity of 3D compact FDTD schemes as

$$v(\hat{k}_x, \hat{k}_y, \hat{k}_z) = \frac{\omega}{\hat{k}\,c} = \frac{2\arcsin\left(\lambda\sqrt{F(s_x, s_y, s_z)}\right)}{\lambda\sqrt{(\hat{k}_x X)^2 + (\hat{k}_y X)^2 + (\hat{k}_z X)^2}}. \tag{17}$$

5. SPECIAL CASES

The choice of the free parameters a, and b (the value of c then follows) determines special cases of 3D FDTD schemes based on a rectilinear grid, and a list of the main ones is provided in Table 1, which also presents the top value of the Courant number and the lowest cutoff frequency (used in ensuing sections). Let us first consider a family of explicit schemes which is obtained by setting $a = 0$. The 3D standard leapfrog (SLF) scheme results for $b = 0$ and $c = 0$ (see stencil in Fig. 1), and for its top Courant number value it is mathematically equivalent to the 3D rectilinear digital waveguide mesh (DWM), and also has the same numerical dispersion and stability characteristics as the 3D Yee's scheme. The octahedral (OCTA) scheme (that is also equivalent to the octahedral DWM) [3, 4] uses an eight-point stencil located in diagonal directions and the stencil

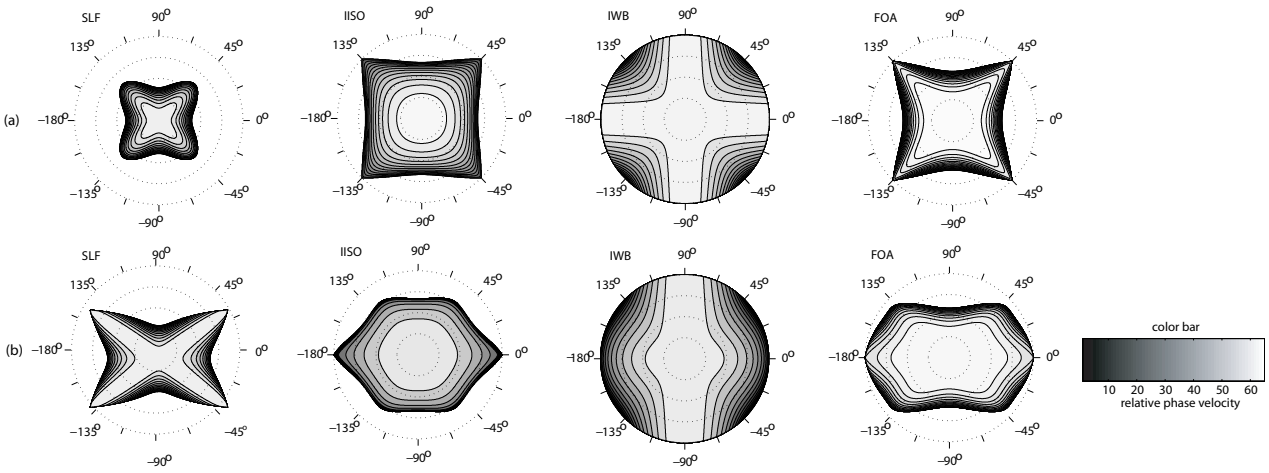

Fig. 2. Relative phase velocity as a function of frequency (polar plot radius) and propagation angle (polar plot angle) for: (a) the horizontal cross section of a cube and (b) the diagonal cross section of a cube. In each plot, starting from the most inner circle, the dotted-line circles indicate $f = (\frac{1}{8}, \frac{1}{4}, \frac{3}{8}, \frac{1}{2})f_s$. For acronyms, refer to Section 5.

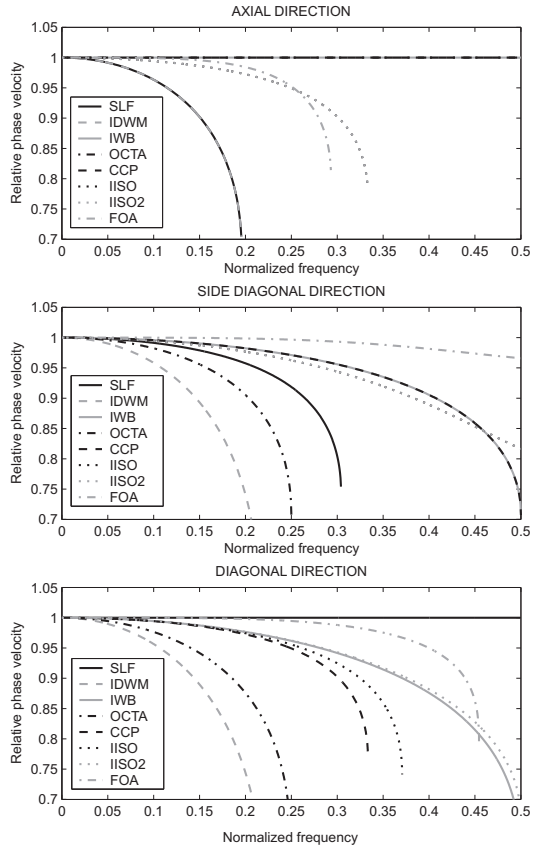

Fig. 3. Relative phase velocity of compact 3D schemes for axial (top), side-diagonal (middle), and diagonal directions (bottom), respectively. Note that in the top plot, the relative phase velocity of the following groups (IWB,OCTA,CCP), (IISO and IISO2), and (SLF,IDWM) overlap, respectively.

of the cubic close-packed (CCP) scheme consists of twelve side-diagonal grid points, as illustrated respectively in Fig. 1. The remaining explicit schemes can, after [3], be classified as 'interpolated schemes', i.e., using a combination of the three aforementioned stencils, as depicted in Fig. 1. Particularly interesting special cases include interpolated isotropic schemes (for which the dispersion error is almost directionally independent), their abbreviations are respectively given as IISO and IISO2, and the only scheme that provides full simulation bandwidth in all propagation directions - the interpolated wideband (IWB) scheme. The 3D interpolated digital waveguide mesh (IDWM) is also compared, for which parameters equivalent to those given in Table 1 have been calculated by optimization up to $0.25f_s$ in [5]. Compact implicit schemes result for $a \neq 0$, and the most accurate special case (originally proposed in [11]) is obtained for the following set of parameters: $a = \frac{1-\lambda^2}{12}$ and $b = \frac{1}{6}$. Contrary to all explicit schemes which are at most second-order accurate, this implicit scheme achieves the forth-order accuracy, and hence it will be referred here as the FOA scheme.

6. DISPERSION ANALYSIS

The relative phase velocity as a function of frequency [calculated with (17)] for four selected grid topologies is depicted in Fig. 2. The SLF scheme (and hence also the 3D DWM and the Yee's scheme) exhibits the highest dispersion in axial directions and has no dispersion in diagonal directions. The IISO scheme has nearly round characteristic in all propagation directions. The IWB scheme displays a full frequency range with a perfect approximation in axial directions; however, its numerical error is rather direction-dependent. The FOA scheme is highly accurate for the widest frequency range but it has quite low cutoff frequencies in axial directions.

As can be seen from Fig. 2, the best and worst approximation always occurs in one of the three extreme propagation directions (i.e., the axial, the side-diagonal, and the diagonal direction of a cube), and thus the exact values of the dispersion error in aforementioned directions for all investigated special cases are depicted in Fig. 3. Note that the lowest cutoff indicates the frequency above which the solutions become heavily damped, hence it determines the

effective frequency range for which a simulation can be considered valid (for the exact values see Table 1). As shown in Fig. 3, the IISO and IISO2 schemes are in general accurate for wider frequency ranges than the OCTA and CCP schemes, the latter additionally suffer from a strongly direction-dependent dispersion error. The IWB scheme has a smaller relative phase velocity error than any other explicit scheme but the FOA scheme proves to be the most accurate of all compact schemes when considering the widest band in which only a very small relative error is admissible (e.g., up to 1%). On the other hand, the most basic SLF scheme performs rather badly compared with other finite-difference schemes. In particular, considering an accuracy range as a frequency band in which the relative phase velocity error does not exceed the value of 2% in any propagation direction, the following results are obtained: $0.075f_s$ for the SLF, $0.093f_s$ for the OCTA, $0.175f_s$ for the CCP, $0.069f_s$ for the IDWM, $0.175f_s$ for the IISO and the IISO2, $0.269f_s$ for the IWB, and $0.214f_s$ for the FOA scheme.

7. ROOM IMPULSE RESPONSE ANALYSIS

To show the implications of the dispersion error on the numerically calculated room impulse response (RIR), a cubic room that consists of 7x7x7, 9x9x9, 10x10x10, and 12x12x12 grid points for schemes respectively having the stability bound at $\lambda = 1/\sqrt{3}, \sqrt{3}-1, \sqrt{3/4}$, and 1 is modeled. Excitation and pickup points are located in the opposite corners, and the boundary nodes are assigned a constant value of zero so that the influence of the boundary is excluded and the numerical results could be compared with theoretical room modes calculated from a simple eigenmode model for rigid boundaries [8].

The comparison of the RIR for the three best performing schemes (i.e., IISO, IWB, and FOA schemes) in comparison with the SLF scheme is illustrated in Fig. 4. A general conclusion can be made that the numerical simulation brings about systematic shifts in modal frequencies which increase with frequency. The SLF scheme has a strongly compressed frequency spectrum, in which only a few pronounced room modes are evident, and in addition the spectrum is symmetric around $0.25f_s$. The IISO scheme performs considerably better, but still suffers from the presence of a fairly low numerical cutoff in axial directions, which leads to an increased modal density around $f = 0.37f_s$. The IWB scheme results in a more gradual increase of modal density, effectively 'pulling in' modes from above Nyquist. Finally, the FOA scheme yields the most accurate approximation at low frequencies. In comparison to the IWB and the IISO, the FOA scheme does not lead to artificially high modal densities. The IWB scheme however is the only scheme that does not suffer from numerical cutoffs, i.e. it produces a response at all frequencies up to Nyquist.

8. CONCLUSIONS

In this paper, a family of compact FDTD schemes for solving the 3D wave equation has been investigated and the most accurate approximations suitable for online applications have been indicated. For a tight accuracy criterion, implicit schemes (such as the FOA scheme) are an interesting choice, as the free numerical parameters can be set to achieve high accuracy for the widest frequency range. When an explicit system formulation is sought after, the newly identified interpolated wideband and isotropic schemes are shown to be more accurate than other explicit FDTD schemes and digital waveguide meshes used in previous studies, including rectilinear, octahedral and cubic close-packed topologies [1]. Furthermore, the interpolated wideband scheme appears to be particularly suited to auralization since it is the only compact nonstaggered scheme that provides a full simulation bandwidth."

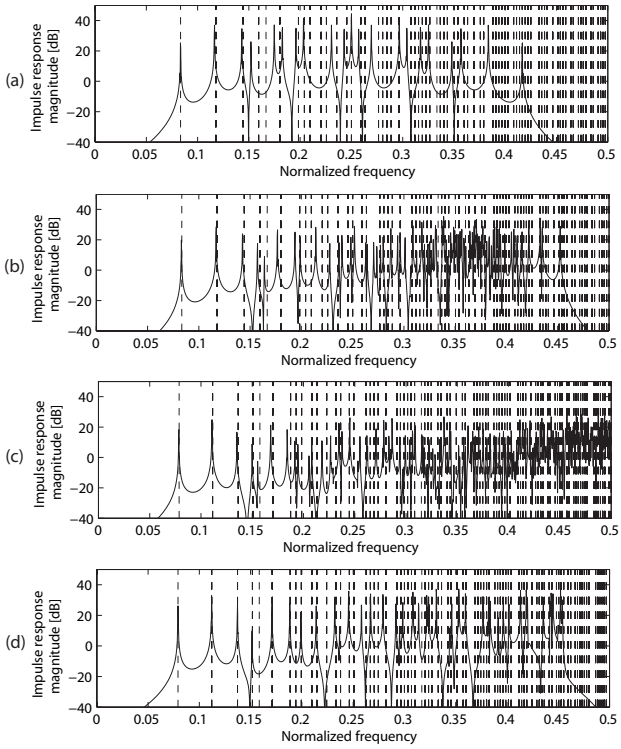

Fig. 4. Magnitude spectrum of the room impulse response for: (a) the SLF scheme, (b) the IISO scheme, (c) the IWB scheme, and (d) the FOA scheme. Dashed lines denote the theoretical mode frequencies of the room.

9. REFERENCES

[1] D. Botteldooren, "Finite-difference time-domain simulation of low-frequency room acoustic problems," *J. Acoust. Soc. Amer.*, vol. 98, no. 6, pp. 3302–3308, 1995.

[2] J.C. Strikwerda, *Finite Difference Schemes and Partial Differential Equations*, Wadsworth & Brooks, Pacific Grove, CA, 1989.

[3] S. Bilbao, *Wave and Scattering Methods for Numerical Simulation*, John Wiley & Sons, London, 2004.

[4] G.R. Campos and D.M. Howard, "On the computational efficiency of different waveguide mesh topologies for room acoustic simulation," *IEEE Trans. Speech Audio Process.*, vol. 13, no. 5, pp. 1063–1072, September 2005.

[5] L. Savioja and V. Välimäki, "Interpolated rectangular 3-D digital waveguide mesh algorithms with frequency warping," *IEEE Trans. Speech Audio Process.*, vol. 1, no. 6, pp. 738–790, November 2003.

[6] S. Bilbao and J.O. Smith, "Finite difference schemes and digital waveguide networks for the wave equation: Stability, passivity, and numerical dispersion," *IEEE Trans. Speech Audio Process.*, vol. 11, pp. 255–266, May 2003.

[1] A computational efficiency comparison for the analyzed schemes is presented in [12], which shows that the newly identified schemes are also more efficient computationally compared to other schemes.

[7] A.R. Gourlay and A.R. Mitchell, "A classification of split methods for hyperbolic equations in several space dimensions," *SIAM J. Numerical Analysis*, vol. 6, no. 1, pp. 62–71, March 1969.

[8] H. Kuttruff, *Room Acoustics*, Applied Science Publishers Ltd, London, 1973.

[9] A. Taflove and S.C. Hagness, *Computational Electrodynamics: The Finite-Difference Time-Domain Method, 2nd ed.*, Artech House, Norwood, MA, 2000.

[10] M. van Walstijn and K. Kowalczyk, "On the numerical solution of the 2D wave equation with compact FDTD schemes," *Proc. Int. Conf. Digital Audio Effects (DAFx'08)*, pp. 205–212, September 2008, Espoo, Finland.

[11] G. Fairweather and A.R. Mitchell, "A high accuracy alternating direction method for the wave equation," *J. Inst. Math. Appl.*, vol. 1, pp. 309–316, May 1965.

[12] K. Kowalczyk, *Boundary and medium modelling using compact finite difference schemes in simulations of room acoustics for audio and architectural design applications*, Ph.D. thesis, Queen's University, Belfast, UK, November 2008.